

Article - Human and Animal Health

Antibacterial and Cytotoxic Activities of Copper-Functionalized Silsesquioxane 3-*n*-Propylpyridinium Chloride

Flávia de Brito Pedroso¹

<https://orcid.org/0000-0002-3533-8867>

Deize Basílio dos Santos de Aguiar¹

<https://orcid.org/0000-0002-2059-6871>

Priscilla Salles de Brito¹

<https://orcid.org/0000-0002-1419-8711>

Christiana Andrade Pessôa²

<https://orcid.org/0000-0001-8973-5908>

Sérgio Toshio Fujiwara² (in memoriam)

<https://orcid.org/0000-0001-5887-7575>

Carla Cristine Kanunfre³

<https://orcid.org/0000-0002-2865-3084>

Ruben Aucçaise Estrada⁴

<https://orcid.org/0000-0002-9602-6533>

Sivaldo Baglie¹

<https://orcid.org/0000-0002-4688-6463>

Jessica Mendes Nadal^{1,*}

<https://orcid.org/0000-0002-2419-2110>

Andressa Novatski⁴

<https://orcid.org/0000-0002-8327-6285>

Paulo Vitor Farago¹

<https://orcid.org/0000-0002-9934-4027>

Alessandro Dourado Loguércio⁵

<https://orcid.org/0000-0001-9880-4856>

¹Universidade Estadual de Ponta Grossa, Departamento de Ciências Farmacêuticas, Programa de Pós-Graduação em Ciências Farmacêuticas, Ponta Grossa, Paraná, Brasil; ²Universidade Estadual de Ponta Grossa, Departamento de Química, Programa de Pós-Graduação em Química, Ponta Grossa, Paraná, Brasil; ³Universidade Estadual de Ponta Grossa, Departamento de Biologia Geral, Programa de Pós-Graduação em Ciências Biomédicas, Ponta Grossa, Paraná, Brasil; ⁴Universidade Estadual de Ponta Grossa, Departamento de Física, Ponta Grossa, Paraná, Brasil; ⁵Universidade Estadual de Ponta Grossa, Departamento de Odontologia, Programa de Pós-Graduação em Odontologia, Ponta Grossa, Paraná, Brasil.

Editor-in-Chief: Yasmine Mendes Pupo
Associate Editor: Jane Manfron Budel

Received: 28-Mar-2022; Accepted: 12-Jun-2022.

*Correspondence: jessicabem@hotmail.com; Tel.: +55 42 991060889 (J.M.N.)

HIGHLIGHTS

- Silsesquioxane 3-*n*-propylpyridinium chloride (SiPy⁺Cl⁻) was synthesized.
- Copper functionalization of SiPy⁺Cl⁻ was performed to obtain Cu-SiPy⁺Cl⁻.
- Antimicrobial and cytotoxic effects of SiPy⁺Cl⁻ and Cu-SiPy⁺Cl⁻ were demonstrated.
- Cu-SiPy⁺Cl⁻ shows a promising use in oral care products.

Abstract: Silsesquioxane 3-*n*-propylpyridinium chloride (SiPy⁺Cl⁻) is a water-soluble polymer that can be used as a promising material with remarkable biological effects. SiPy⁺Cl⁻ can form thin films on substrate surfaces and shows suitable adhesiveness. Besides, it has high affinity for metal ions. Considering this effect as exchanger polymer and the well-known antimicrobial and cytotoxic features of copper, the aim of this study was to perform the copper functionalization of silsesquioxane 3-*n*-propylpyridinium chloride Cu-SiPy⁺Cl⁻. The

SiPy⁺Cl⁻ was obtained by the sol-gel processing method and the incorporation of copper (II) chloride was carried out by immobilization. Its characterization was performed by spectroscopic methods of Fourier-transform infrared spectroscopy (FTIR) and nuclear magnetic resonance (NMR). The FTIR spectrum of SiPy⁺Cl⁻ showed symmetric and asymmetric stretching of Si-O-Si group and also exhibited vibrational bands of pyridinium ring. The FTIR spectrum of Cu-SiPy⁺Cl⁻ assigned typical bands displacements of the metal coordination to nitrogen atoms. Spectroscopic data recorded by ¹³C and ²⁹S NMR confirmed the chemical structures of SiPy⁺Cl⁻ and Cu-SiPy⁺Cl⁻. Concerning to the in vitro susceptibility assay, the antimicrobial activity against *Staphylococcus aureus*, *Escherichia coli* and *Streptococcus mutans* was achieved by the agar-well diffusion method. Cu-SiPy⁺Cl⁻ showed similar cytotoxicity than SiPy⁺Cl⁻ against Calu-3 and 3T3 cell lines by the MTT colorimetric assay. Further studies are required to investigate the use of Cu-SiPy⁺Cl⁻ as a novel dental material.

Keywords: antimicrobial activity; cell viability; copper functionalization; novel dental materials.

INTRODUCTION

Silsesquioxane 3-*n*-propylpyridinium chloride (SiPy⁺Cl⁻) is a water-soluble and film-forming polymer. SiPy⁺Cl⁻ can form a stable thin film on substrate surfaces such as aluminum oxide, cellulose fibers, silica gel, and glass surfaces [1,2]. This organosilicate also shows suitable adhesion and ion adsorption features, which provide highly desirable multifunctional physicochemical properties and remarkable applications [3]. Some studies have investigated its use as adsorbent material [4] for preparing electrodes [5,6] and sensors [7]. Besides, SiPy⁺Cl⁻ can undergo structural changes for obtaining organic-inorganic hybrid compounds, which play an important role in providing a chemical platform for discovery of novel materials [3].

The development of low costing, safe, and effective antimicrobial products for hygienic, dental, or medical purposes in textiles, devices, and surgical instruments is of growing interest [3]. Recent studies in microbiology have focused on copper and its use as antimicrobial ion in health care [8]. The antimicrobial effect of copper has been well known [9] by contributing to the reactive oxygen species formation and inducing lipid peroxidation in bacterial membranes. Also, the disruption of bacterial enzymes and cell membranes can be achieved by positively charged polymers, with less susceptibility of bacterial resistance and cytotoxicity [10].

In that sense, the broad-spectrum antimicrobial properties of a novel organic-inorganic hybrid compound containing the SiPy⁺Cl⁻ organosilicate and the copper seems to be an innovative improvement in the battle against health care-associated infections [8]. However, to the best of our knowledge, no previous paper was devoted to study the copper-functionalized SiPy⁺Cl⁻ and its antimicrobial and cytotoxic in vitro effects since this novel compound may be further used for improving the clinical performance of antibacterial supplies for health and oral care [11].

The aim of this study was to perform the synthesis and the characterization of a copper-functionalized silsesquioxane 3-*n*-propylpyridinium chloride in order to investigate its in vitro antibacterial and cytotoxic properties.

MATERIAL AND METHODS

Synthesis of silsesquioxane 3-*n*-propylpyridinium chloride

The silsesquioxane compound known as SiPy⁺Cl⁻ was prepared by the sol-gel processing method [5]. In brief, the synthesis consisted of the acid prehydrolysis of tetraethyl orthosilicate (Sigma-Aldrich, St. Louis, MO, USA) in water-ethanol solution followed by the incorporation of the pyridinium organic group (pyridine anhydrous, 99.8% pure, Sigma-Aldrich, St. Louis, MO, USA) according to the procedure previously described in the literature [12,13]. All reagents were analytical grade with no further purification. The water-ethanol solution was prepared with water from a Millipore Milli-Q system (Merck Group, Darmstadt, Germany). The schematic procedure to obtain the ion exchanger polymer is summarized in Figure 1.

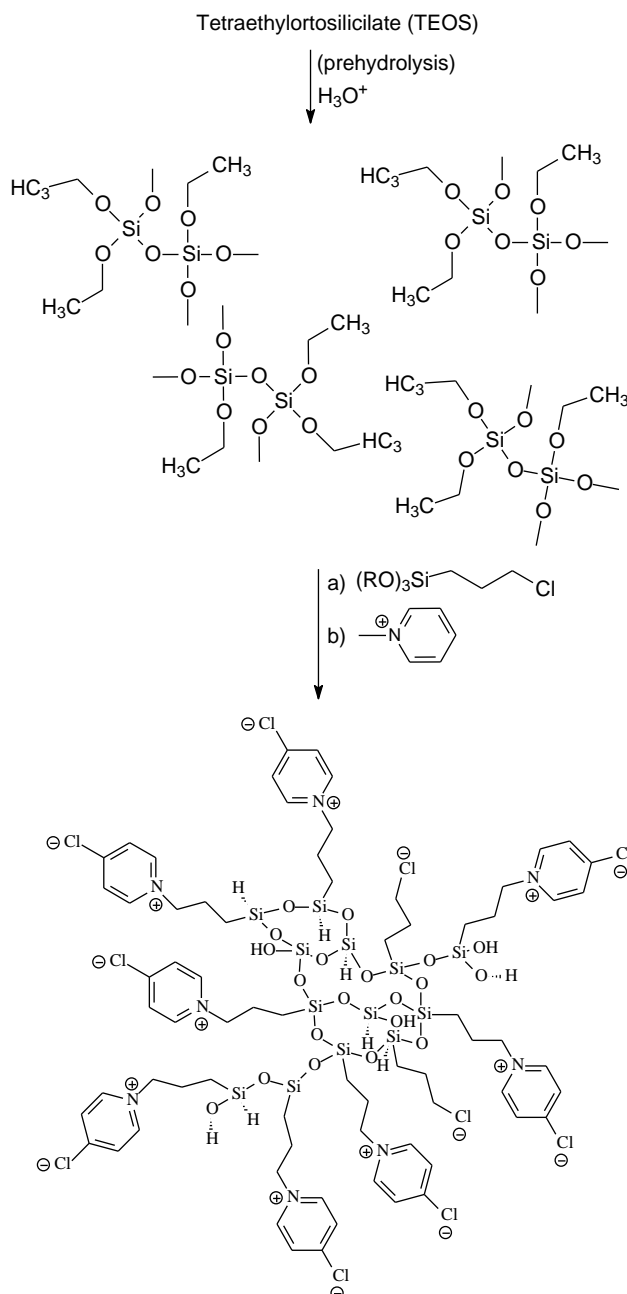


Figure 1. Synthesis scheme of the silsesquioxane 3-*n*-propylpyridinium chloride.

Copper functionalization of silsesquioxane 3-*n*-propylpyridinium chloride

The incorporation of copper (II) chloride into SiPy⁺Cl⁻ was performed by immobilization considering that the exchange capacity of SiPy⁺Cl⁻ is 2.8 mmol.g⁻¹, which allows the immobilization of 1.4 mmol.g⁻¹ of Cu²⁺. The SiPy⁺Cl⁻ organosilicate (1.007 g, 0.2 mmol.g⁻¹) was weighed and was added to the aqueous copper (II) chloride solution (0.237 g of CuCl₂.2H₂O, 0.1 mmol.g⁻¹, MW = 170.48 g.mol⁻¹). The final solution was magnetically stirred at room temperature (20 ± 2°C) for 48 h to obtain the copper-functionalized product Cu-SiPy⁺Cl⁻.

Characterization of copper-functionalized silsesquioxane 3-*n*-propylpyridinium chloride

Fourier-transform infrared spectroscopy (FTIR)

The Fourier-transform infrared spectra of SiPy⁺Cl⁻ and Cu-SiPy⁺Cl⁻ were recorded from 4000 to 400 cm⁻¹ on a Shimadzu IR Prestige-21 spectrophotometer (Kyoto, Japan) using KBr pellets with 32 scans and resolution of 4 cm⁻¹.

Nuclear magnetic resonance (NMR) spectroscopy

For structural elucidation, solid state ^{13}C and ^{29}Si NMR experiments were performed on a Bruker 400 MHz spectrometer (Bremen, Germany) using a standard Magic Angle Spinning (MAS) probe 4 mm at room temperature. The strong static magnetic field is $B_0 = 9.4\text{ T}$ and the corresponding resonant frequencies for ^{29}Si , ^{13}C , and ^1H were 79.488 MHz, 100.625 MHz, and 400.132 MHz, respectively. The SiPy^+Cl^- and $\text{Cu-SiPy}^+\text{Cl}^-$ samples were placed on zirconia rotors and were spun at 13 kHz.

The ^{13}C NMR spectra were obtained using the Variable Amplitude Cross Polarization-Magic Angle Spinning (VACP-MAS) technique. The main parameter values of this pulse sequence were the contact time of 1 ms, the recycle time delay of 3 s, the number of scans of 20,400; and the acquisition time of 15.98 ms. The external pattern used was the CH_2 carbon of the glycine ($\delta_{\text{iso}} = 43.5\text{ ppm}$) [14].

The ^{29}Si spectra were obtained using Direct Polarization-Magic Angle Spinning (DP-MAS) NMR using as the main parameter values: the time pulse of 2 μs , the recycle time delay of 1 s, the number of scans of 76,400; and the acquisition time of 16.58 ms. The external pattern used was kaolinite ($\delta_{\text{iso}} = -91.5\text{ ppm}$) [15].

In vitro antibacterial screening assay

The antimicrobial potential of SiPy^+Cl^- and $\text{Cu-SiPy}^+\text{Cl}^-$ was investigated using agar-well diffusion method. Tests were carried out in triplicate containing $n = 5$ per assay and the chlorhexidine digluconate (Sigma-Aldrich, St. Louis, MO, USA) was used as positive control. For *Streptococcus mutans* (ATCC 25,175), plates containing Mueller-Hinton agar with 5% sheep blood were inoculated with the bacterial strains from a previously standardized inoculum suspension at $5 \times 10^5\text{ CFU.mL}^{-1}$ that achieved the turbidity of the 0.5 McFarland standard by swab streaking. Wells of 7 mm diameter were placed on agar plates and 0.5, 1.0; and 2.0% of SiPy^+Cl^- and $\text{Cu-SiPy}^+\text{Cl}^-$ were added to the wells [16,17]. These plates were incubated under microaerophilic conditions for 24 h at $35 \pm 0.5^\circ\text{C}$. For *Escherichia coli* (ATCC 25,925) and *Staphylococcus aureus* (ATCC 25,923), the assays were performed in sterile Müller-Hinton agar and under aerobic conditions [18]. The zone of growth inhibition was measured in millimeters. One-way ANOVA with Tukey's post-hoc test ($p < 0.05$) for multiple comparison was used considering the mean growth inhibition zone diameter resulted from the antibacterial activity.

In vitro cell culture-based assay

Cell culture

Calu-3 and 3T3 cell lines were cultured in RPMI 1640 medium at pH 7.4 containing 5% fetal bovine serum, supplemented with 24 mmol.L^{-1} sodium bicarbonate, 2 mmol.L^{-1} L-glutamine, 1 mmol.L^{-1} sodium pyruvate, $10,000\text{ U.L}^{-1}$ penicillin, and 10 mg.L^{-1} streptomycin. Cultures were maintained in a humidified oven at 37°C with 5% CO_2 atmosphere.

Cell treatment

Calu-3 and 3T3 cells were seeded in 96-well plates at a density of $1.5 \times 10^4\text{ cells.well}^{-1}$ and incubated for 24 h in culture medium. For evaluating the cytotoxicity, cell lines were incubated with the samples SiPy^+Cl^- and $\text{Cu-SiPy}^+\text{Cl}^-$ at 50, 250, 500, 1000, and 2000 $\mu\text{g.mL}^{-1}$ for 72 h at 37°C with 5% CO_2 atmosphere. Tests were obtained using serial dilution procedure (when possible) and were performed as four independent experiments containing $n = 4$ per assay.

Cell viability by methylthiazolyldiphenyl-tetrazolium bromide (MTT) test

After 72 h of the treatments, 200 μL of a MTT solution at 0.5 mg.mL^{-1} was added to the wells following a standard method [19]. The cultures were then incubated at 37°C for 2 h, protected from light, until the presence of formazan crystals. The supernatant was then removed. For the solubilization of these crystals, 200 μL of dimethyl sulfoxide was added [20]. The spectrophotometric absorbance reading was performed at a wavelength of 550 nm in a μQuant microplate reader (BioTek, Winooski, VT, USA). In order to calculate the cell viability, Equation 1 was used.

$$\text{Cell viability (\%)} = \frac{\text{absorbance of test}}{\text{absorbance of control}} \times 100 \quad (1)$$

RESULTS AND DISCUSSION

Synthesis and characterization of silsesquioxane 3-*n*-propylpyridinium chloride and copper-functionalized silsesquioxane 3-*n*-propylpyridinium chloride

The SiPy⁺Cl⁻ synthesis and its copper functionalization to obtain Cu-SiPy⁺Cl⁻ were successfully performed. These materials showed powder aspect with white and bright yellow colors, respectively. These compounds were then characterized by FTIR and NMR in order to confirm their chemical structures.

Fourier-transform infrared spectroscopy (FTIR)

FTIR spectra performed for SiPy⁺Cl⁻ and Cu-SiPy⁺Cl⁻ are shown in Figure 2. The FTIR spectrum consisted of absorption bands that shows an intense and wide band at 1,082 cm⁻¹ and two other bands at 775 cm⁻¹ and 457 cm⁻¹ that are assigned respectively to the asymmetric and symmetrical stretch mode of the Si-O-Si skeleton and the SiOSi deformation mode of the Si-O-Si group [21]. The spectrum also shows the vibrational bands characteristic of the pyridinium ring in 1633 and 1489 cm⁻¹, whose values are similar to those presented in the literature [22]. The FTIR spectrum of Cu-SiPy⁺Cl⁻ presented bands of the pyridinium ring showed a displacement, from 1633 and 1489 cm⁻¹ to 1631 and 1483 cm⁻¹, respectively. These changes are typical of the coordination of the metal to the nitrogen atoms.

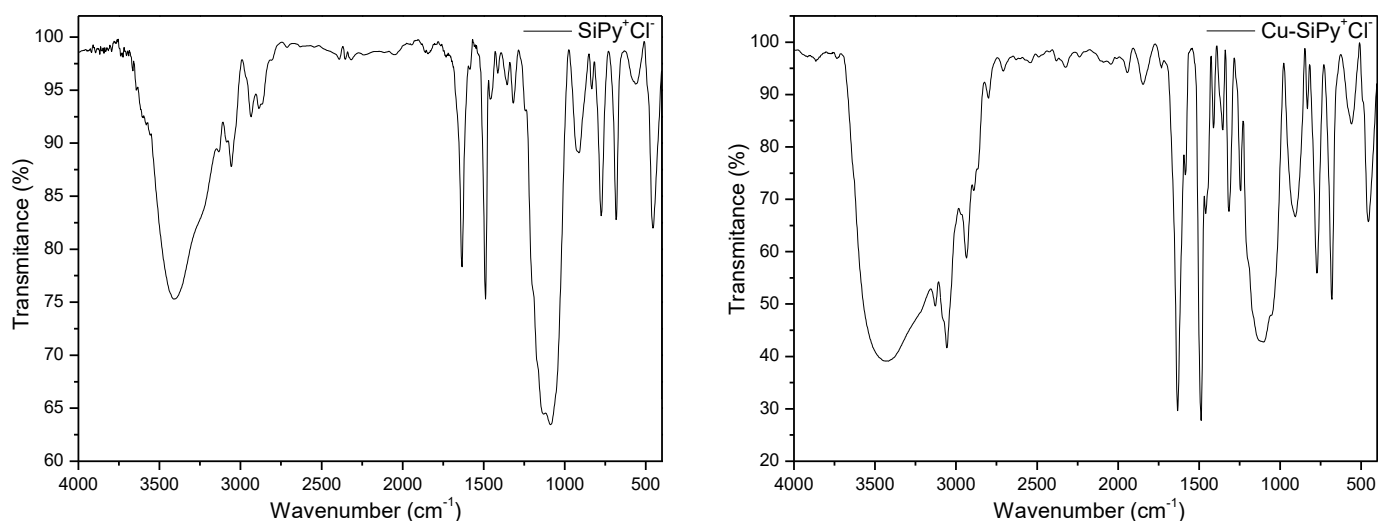


Figure 2. FTIR spectra of SiPy⁺Cl⁻ and Cu-SiPy⁺Cl⁻

Nuclear magnetic resonance spectroscopy

The ¹³C and ²⁹S NMR spectral data confirmed the chemical structure of SiPy⁺Cl⁻ and its functionalization with copper.

The ¹³C solid-state NMR spectra for SiPy⁺Cl⁻ and Cu-SiPy⁺Cl⁻ are depicted in Figure 3. The main chemical shifts for carbon signals were identified and labeled as C_{1,2,3,3'} and C_{α,β,γ} following the cartoon sketched at the top of Figure 3. The signal at 10.26 ppm (and its shifted counterpart at 18.02 ppm) was associated to the C₁ carbon which was near to the Si nuclei and the peak at 26.72 (and its shifted counterpart at 31.40 ppm) corresponded to the C₂ carbon flanked on both sides by two carbon nuclei [1,21].

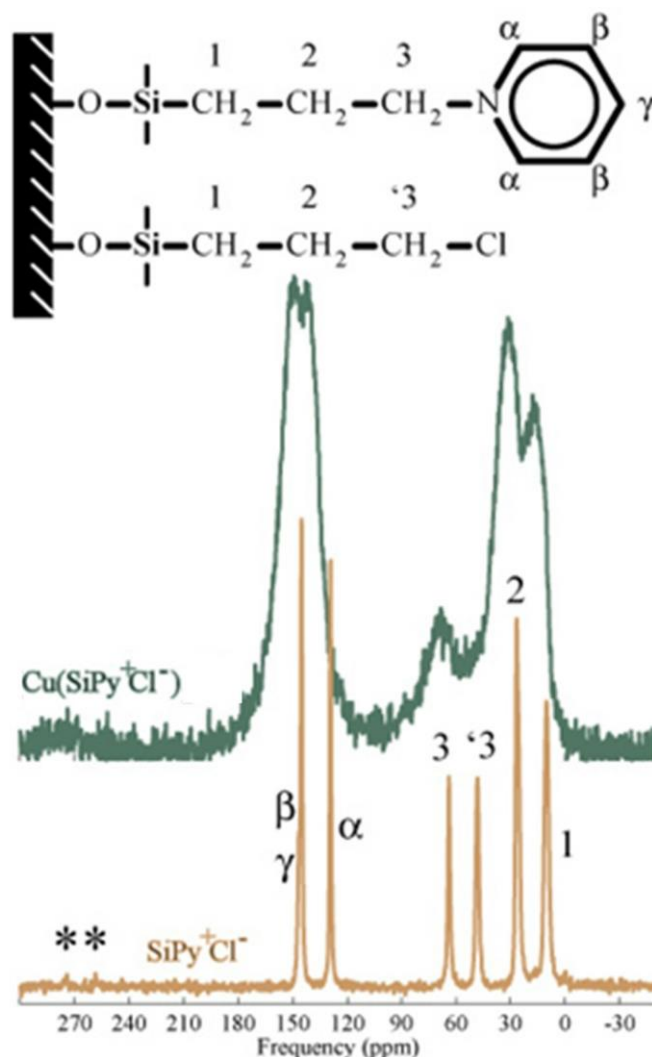


Figure 3. The cartoon of the structural formula of the molecules related to the ^{13}C chemical environments was sketched at the top. At the middle and at the bottom, the solid state ^{13}C (VACP-MAS) NMR spectra of $\text{Cu-SiPy}^+\text{Cl}^-$ and SiPy^+Cl^- samples were displayed, respectively. The asterisk symbol represented the spinning sidebands.

The peak at 63.94 ppm (and its shifted counterpart at 68.20 ppm) was attributed to the modifier function at the C_3 carbon directly attached to nitrogen and the peak at 48.26 ppm corresponded to the C_3 carbon of the 3-chloropropyl group bonded to silicon polymer [21,23]. The presence of this signal was an indication that a small proportion of unreacted chloropropyl groups was still present in the SiPy^+Cl^- silsesquioxane [21].

The signal value at 129 ppm (and its shifted counterpart at 142.90 ppm) was related to both C_α carbons and the signal value at 145.10 ppm (and its shifted counterpart at 149.30 ppm) was assigned to both C_β carbons and C_γ carbon [1,21]. Those ^{13}C chemical shifts are summarized in Table 1.

Table 1. ^{13}C chemical shifts of SiPy^+Cl^- and $\text{Cu-SiPy}^+\text{Cl}^-$ samples

Chemical environment	Chemical shift (ppm)			
	SiPy^+Cl^-	$\text{Cu-SiPy}^+\text{Cl}^-$	Reference [21]*	Reference [1]*
1	10.26	18.02	9.4	10
2	26.72	31.40	25.4	26
'3	48.26	—	—	49
3	63.94	68.20	63.9	65
A	129.10	142.90	129.2	129
β, γ	145.10	149.30	145.1	145

* The carbon labeling was related to the cartoon molecule at the top of Figure 3. The chemical shifts were supported by previous reports discussing similar (not the same) chemistry developments.

A downfield, broad line and noise effects were highlighted as another collective signature of the ^{13}C chemical shifts of $\text{Cu-SiPy}^+\text{Cl}^-$ sample. Those effects were generated by the proximity of electronegative atoms in the bonding network. Any radical atom, molecule or ion (in this case the Cu^{2+} ions) induced a chemical shift of the spectral lines (in this case, the spectral lines were shifted at the left of the spectrum) [24].

Typical ^{29}Si NMR spectra of SiPy^+Cl^- and $\text{Cu-SiPy}^+\text{Cl}^-$ are presented in Figure 4. Their observed peaks are showed in Table 2. The observed ^{29}Si chemical shifts for both samples were assigned to the silicon (bold character) in the following environments: the ^{29}Si signal of the chemical environment $\text{R-Si}(\text{OR}')(\text{OH})(\text{OSi}\equiv)$ labeled by T_2 was identified at -49.87 ppm [1]; The ^{29}Si signal of the chemical environment $\text{R-Si}(\text{OH})(\text{OSi}\equiv)_2$ labeled by T_3 was identified at -58.56 ppm; the ^{29}Si signal of the chemical environment $\text{R-Si}(\equiv\text{SiO})_3$ unit of silsesquioxane cluster labeled by T_4 was identified at -67.85 ppm. Those chemical shifts were related to chemical environments of the T's kind for the ^{29}Si nuclei.

Three chemical environments of the Q's kind were also observed. The chemical environment $(\equiv\text{SiO})_2\text{Si}(\text{OH})_2$ was labeled as Q_2 at -91.75 ppm. The main two peaks at -101.3 and -110.8 ppm were attributed to pure surface signals and corresponded to the chemical environments $(\equiv\text{SiO})_3\text{Si}(\text{OH})$ and $(\equiv\text{SiO})_4\text{Si}$ labeled as Q_3 and Q_4 , respectively [13].

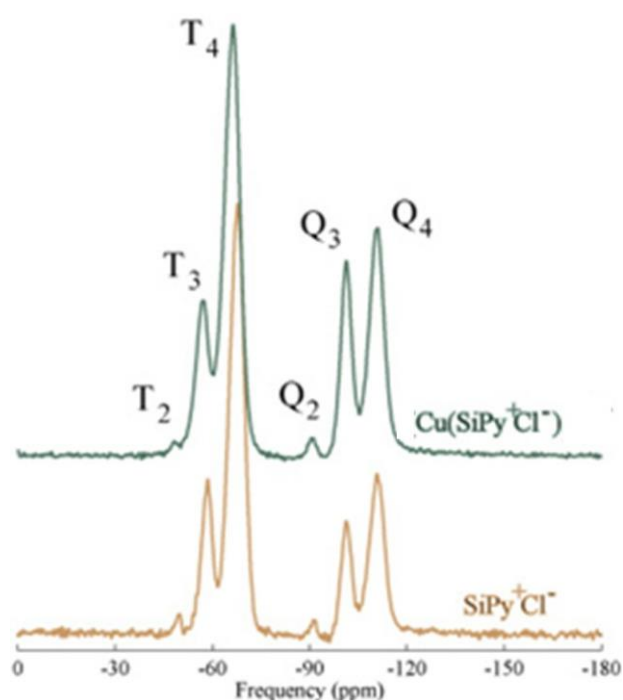


Figure 4. At the top and at the bottom, the solid state ^{29}Si (DP-MAS) NMR spectra of $\text{Cu-SiPy}^+\text{Cl}^-$ and SiPy^+Cl^- samples was displayed, respectively.

Table 2 ^{29}Si chemical shifts of SiPy^+Cl^- and $\text{Cu-SiPy}^+\text{Cl}^-$ samples

Chemical Environment	Chemical Shift (ppm)				
	SiPy^+Cl^-	$\text{Cu-SiPy}^+\text{Cl}^-$	Reference [13]*	Reference [1]*	Reference [21]*
T_2	-49.87	-48.20		-49	-50
T_3	-58.56	-57.10	-57	-58	-59
T_4	-67.85	-66.35	-65	-68	-68
Q_2	-91.75	-90.80		-86*	-91
Q_3	-101.30	-101.30	-101	-101	-101
Q_4	-110.80	-111.00	-110	-110	-111

* The silicon labeling and chemical shifts were supported by previous reports discussing similar (not the same) chemistry developments.

In vitro antibacterial screening assay

The antibacterial activity of SiPy⁺Cl⁻ and Cu-SiPy⁺Cl⁻ was evaluated against gram-positive and gram-negative bacteria using the well diffusion method. The zones of total growth inhibition expressed in millimeters (mean \pm standard deviation) at different concentrations are summarized in Table 3 and Table 4, respectively.

Table 3. Antibacterial activity of SiPy⁺Cl⁻ by the agar well diffusion method.

	SiPy ⁺ Cl ⁻ (%)			
	0.5	1.0	2.0	Positive Control
<i>Staphylococcus aureus</i>	8.66 \pm 1.15 ^b	12.33 \pm 0.58 ^a	13.67 \pm 1.15 ^a	19.66 \pm 0.58
<i>Escherichia coli</i>	12.67 \pm 1.52 ^a	18.00 \pm 1.00 ^b	22.33 \pm 0.60 ^c	20.00 \pm 0.00
<i>Streptococcus mutans</i>	11.56 \pm 0.57 ^a	15.67 \pm 0.58 ^b	18.00 \pm 1.00 ^c	19.66 \pm 0.58

*Results were expressed as mean inhibition zone (IZ) diameter (mm) \pm SD of independent experiments in triplicate. Different letters indicated a statistically significant difference ($p < 0.05$) between the IZ diameters for the studied bacterial stains.

Table 4. Antibacterial activity of Cu-SiPy⁺Cl⁻ by the agar well diffusion method.

	Cu-SiPy ⁺ Cl ⁻ (%)			
	0.5	1.0	2.0	Positive Control
<i>Staphylococcus aureus</i>	10.67 \pm 0.58 ^a	11.33 \pm 1.15 ^a	13.0 \pm 1.64 ^a	19.66 \pm 0.58
<i>Escherichia coli</i>	12.0 \pm 0.60 ^a	19.33 \pm 0.57 ^b	23.0 \pm 1.00 ^c	20.00 \pm 0.00
<i>Streptococcus mutans</i>	12.33 \pm 1.15 ^a	16.00 \pm 1.00 ^b	19.67 \pm 0.57 ^c	19.66 \pm 0.58

*Results were expressed as mean inhibition zone (IZ) diameter (mm) \pm SD of independent experiments in triplicate. Different letters indicated a statistically significant difference ($p < 0.05$) between the IZ diameters for the studied bacterial stains.

In general, SiPy⁺Cl⁻ and Cu-SiPy⁺Cl⁻ provided a remarkable antibacterial effect against the tested bacteria. At the higher concentration (2.0%), the antibacterial activity against *E. coli* and *S. mutans* was similar to those observed for the positive control. The copper functionalization showed no incremental effect on antimicrobial activity. The inhibitory effect on bacterial growth was dose dependent for the three assayed stains.

The quaternary ammonium salt and the copper content can perform bacterial death. SiPy⁺Cl⁻ disrupted cell membrane through the binding of their ammonium cations to anionic sites in the outer layer of bacteria. Copper linked to amino sites positively charged and, i.e., formed protonated amino groups, and was attached to the outer negatively charged lipid membrane and inserted itself into the inner leaflet of bacterial membranes [25]. This interaction disrupted the surrounding lipid layers and triggered the leakage of intracellular content [10,26].

In vitro cell culture-based assays

In order to design novel strategies for the management of microbial adherence and colonization in the oral environment, it is essential to investigate the cytocompatibility of these materials [27,28]. In that sense, Figure 5 represents the cell viability of Calu-3 and 3T3 cell lines in the presence of SiPy⁺Cl⁻ and Cu-SiPy⁺Cl⁻ after 72 h.

SiPy⁺Cl⁻ provided a statistically significant reduction for both Calu-3 and 3T3 cell lines at concentrations of 1000 and 2000 $\mu\text{g}\cdot\text{mL}^{-1}$. The copper functionalization demonstrated the same cytotoxic effect for Cu-SiPy⁺Cl⁻ by reducing the cell viability at 1000 and 2000 $\mu\text{g}\cdot\text{mL}^{-1}$. Thus, the presence of copper did not affect the cytotoxicity in relation to the raw material.

Dental self-etching adhesives are usually toxic to pulp cells by resulting in a 26-35% decrease in cellular metabolic activity. LANZA *et al.* (2009) [29] evaluated through MTT the transdermal diffusion and cytotoxicity of commercially available self-etching adhesives against odontoblastic cells. It was observed that the reduction in cell viability promoted by the self-etching systems ranged from 28-48%.

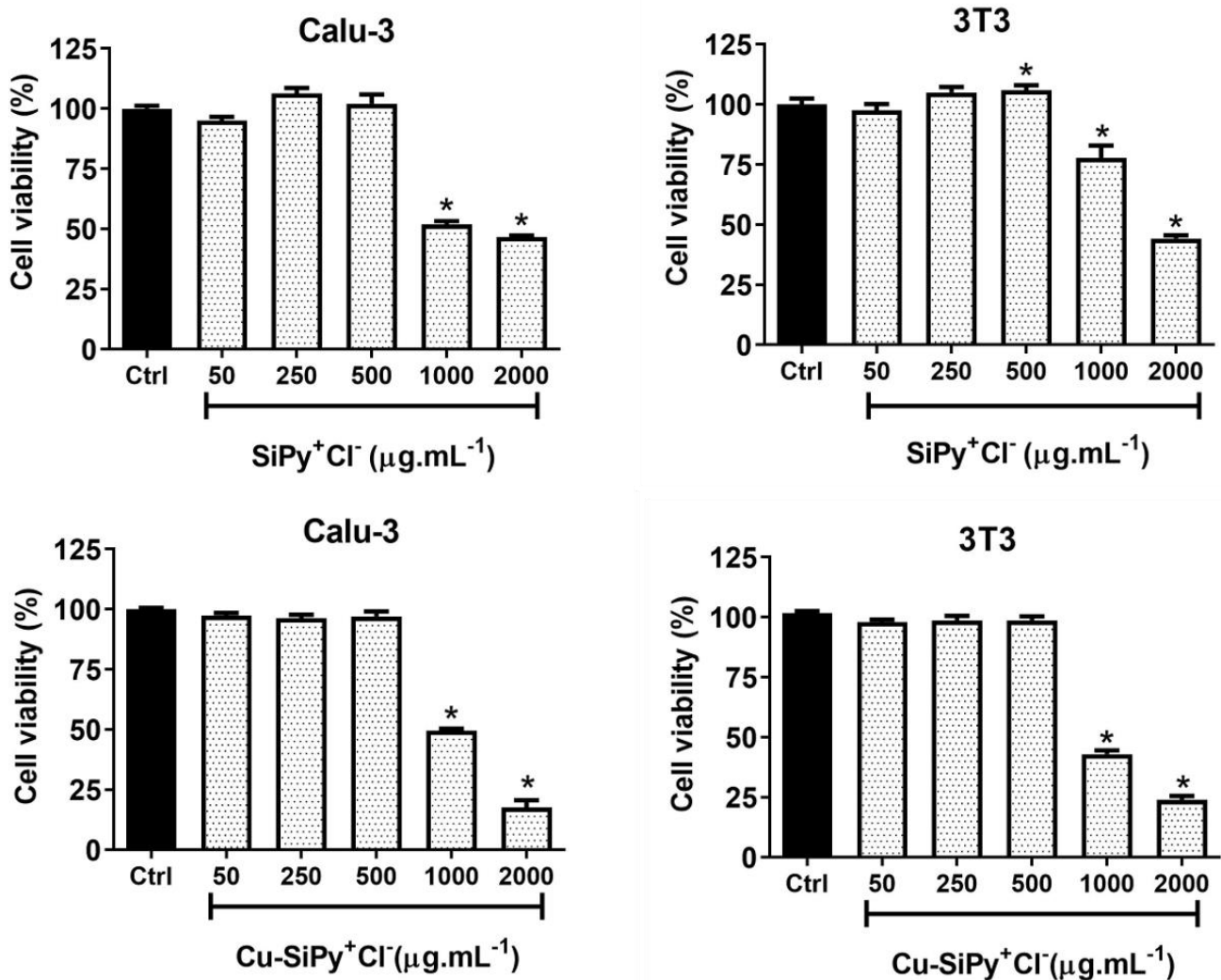


Figure 5. Cell viability of Calu-3 and 3T3 cell lines by MTT assay after their treatment with SiPy⁺Cl⁻ and Cu-SiPy⁺Cl⁻ at different concentrations for 72h.

*Results are expressed as mean \pm standard error of the mean from 4 independent experiments (n=16). Asterisks denote significance levels compared to control, $p < 0.05$.

Several studies have been used to evaluate the cytotoxicity of adhesive systems and their components. These materials should not have harmful effects on dental structures by presenting biocompatibility combined with durability [30] and by preventing bacterial infiltration and seal dental caries [31]. However, direct contact of adhesive systems on the pulp tissue should be avoided due to these materials may cause an intense and persistent inflammatory reaction on the pulp cells [31,32].

Additional cell viability tests of experimental adhesives containing SiPy⁺Cl⁻ and Cu-SiPy⁺Cl⁻ should be performed to assess whether there is leaching of the incorporated compounds and damage to dentin tissue.

CONCLUSION

The synthesis of SiPy⁺Cl⁻ was successfully performed by the sol-gel processing method and the copper functionalization Cu-SiPy⁺Cl⁻ was obtained by immobilization. The chemical structure of both compounds was confirmed by FTIR and ¹³C and ²⁹S NMR spectra.

Cu-SiPy⁺Cl⁻ demonstrated a similar antibacterial potential and cytotoxicity against Calu-3 and 3T3 than SiPy⁺Cl⁻.

SiPy⁺Cl⁻ and Cu-SiPy⁺Cl⁻ can be further used in novel dental material in order to avoid microorganisms with minimal invasive consequences.

Funding: This research was funded by CNPq – Conselho Nacional de Pesquisa e Desenvolvimento, grant number 313704/2019-8.

Acknowledgments: The authors are grateful to CLABMU-UEPG for technical support.

Conflicts of Interest: The authors declare no conflict of interest.

REFERENCES

1. Alfaya RVS, Gushikem Y, Alfaya AA. [Preparation process of 3-n-propylpyridinium chloride polyelectrolyte bound to a silsesquioxane structure], Brazil, Patent INPI No. PI9803053-1, 1998 (BR 9803053-A, 2001), Portuguese.
2. Fujiwara ST, Gushikem Y, Alfaya VS. Adsorption of FeCl₃, CuCl₂ and ZnCl₂ on silsesquioxane 3-n-propylpyridiniumchloride polymer film adsorbed on Al₂O₃ coated silica gel. *Colloids Surf. A Physicochem. Eng. Asp.* 2001;178(1):135-41.
3. Ciriminna R, Fidalgo A, Pandarus V, Béland F, Ilharco LM, Pagliaro M. The Sol-Gel Route to Advanced Silica-Based Materials and Recent Applications. *Chem. Rev.* 2013;113(8):6592–620.
4. Magosso HA, Fattori N, Kholinb YV, Gushikem Y. Adsorption of metal ions on novel 3-n-propyl (methylpyridinium) silsesquioxane chloride polymers surface: study of heterogeneous equilibrium at the solid-solution interface. *J. Braz. Chem. Soc.* 2009;20(4): 744-52.
5. Alfaya RVS, Alfaya AAS, Gushikem Y, Rath S. Ion Selective Electrode for Potentiometric Determination of Saccharin Using a Thin Film of Silsesquioxane 3-n-Propylpyridinium Chloride Polymer Coated-Graphite Rod, *Anal. Lett.* 2000;33(14):2859-71.
6. Muxel AA, de Jesús DA, Alfaya RVS, Alfaya AAS. Silsesquioxane 3-n-Propylpyridinium Chloride: A New Polymer for the Potentiometric Analysis of Cr(VI) in Electroplating and Leather Industry Wastes. *J. Braz. Chem. Soc.*, 2007;18(3),572-6.
7. Fujiwara ST, Pessôa CA, Gushikem Y. Copper (II) tetrasulpho-phthalocyanine entrapped in a propylpyridiniumsilsesquioxane polymer immobilized on a SiO₂/Al₂O₃ surface: use for electrochemical oxidation of ascorbic acid. *Anal. Lett.* 2002;35(7):1117-34.
8. Arendsen LP, Thakar R, Sultan AH. The use of copper as an antimicrobial agent in health care, including obstetrics and gynecology. *Clin. Microbiol. Rev.* 2019;32(4):1-28.
9. Mathews S, Kumar R, Solioz M. Copper Reduction and Contact Killing of Bacteria by Iron Surfaces. *Appl. Environ. Microbiol.* 2015;81(18):6399-403.
10. Jiao Y, Tay FR, Niu, Ln, Chen J-h. Advancing antimicrobial strategies for managing oral biofilm infections. *Int J Oral Sci.* 2019;11(3):28.
11. Armstrong S, Breschi L, Özcan M, Pfefferkorn F, Ferrari M, Meerbeek BV. Academy of Dental Materials guidance on in vitro testing of dental composite bonding effectiveness to dentin/enamel using micro-tensile bond strength (μ TBS) approach. *Dent. Mater.* 2017;33(2):133-43.
12. Gushikem Y, Benvenutti EV, Kholin YV. Synthesis and applications of functionalized silsesquioxane polymers attached to organic and inorganic matrices. *Pure Appl. Chem.* 2008;80(7):1593-611.
13. Ribicki AC, Chemin BG, Van Haandel VJ, Winiarski JP, Rozada TC, Pessoa CA, et al. Sol gel synthesis of 3-n-propyl(4-aminomethyl)pyridinium silsesquioxane chloride and the enhanced electrocatalytic activity of LbL films. *J Sol-Gel Sci Technol.* 2018;87(1):216-229.
14. Ye C, Fu R, Hu J, Hou L, Ding S. Carbon-13 chemical shift anisotropies of solid amino acids. *Magn. Reson. Chem.* 1993;31(8):699-704.
15. Barron PF, Frost RL, Skjemstad JO, Koppi AJ. Detection of two silicon environments in kaolins by solid-state ²⁹Si NMR. *Nature.* 1983;302 (5903):49-50.
16. Pupo YM, Farago PV, Nadal JM, Esmerino LA, Maluf DF, Zawadzki SF, et al. An innovative quaternary ammonium methacrylate polymer can provide improved antimicrobial properties for a dental adhesive system. *J. Biomater. Sci. Polym. Ed.* 2013;24(12):1443-58.
17. Lsi C. Performance standards for antimicrobial susceptibility testing. Clinical Lab Standards Institute, 2016.
18. Ferrari DO, Zanella L, Lund RG, Roman Jr WA, Rodrigues-Junior SA. Hydroalcoholic Extract of *Eugenia uniflora* as Denture Disinfectant: Antimicrobial Activity and Effect on the Physical Properties of Polymethylmethacrylate. *Braz. Arch. Biol. Technol.* 2020;63:e20190704.
19. Molinaro EM, Caputo LFG, Amendoeira MRR. [Concepts and Methods for Training Professionals in Health Laboratories], v. 4: EPSJV 2009.
20. Alper M, Özay C, Güneş H, Mammadov R. Assessment of Antioxidant and Cytotoxic Activities and Identification of Phenolic Compounds of *Centaurea solstitialis* and *Urospermum picroides* from Turkey. *Braz. Arch. Biol. Technol.* 2021;64:e21190530.
21. De Menezes EW, Lima EC, Royer B, de Souza FE, dos Santos BD, Gregório JR, et al. Ionic silica based hybrid material containing the pyridinium group used as an adsorbent for textile dye. *J. Colloid Interface Sci.* 2012;378(1):10-20.
22. Bi Y-T, Li Z-J, Liu T-S. Preparation and characterization of Octa(aminophenyl)silsesquioxane–aldehyde organic/inorganic hybrid aerogel. *Eur. Polym. J.* 2014;58:201-6.
23. Müller CA, Schneider M, Mallat T, Baiker A. Titania–silica epoxidation catalysts modified by polar organic functional groups. *J. Catal.* 2000;189(1):221-32.
24. Jacobsen NE. NMR spectroscopy explained: simplified theory, applications and examples for organic chemistry and structural biology. Chichester: John Wiley & Sons, 2007.

25. Gutiérrez MF, Malaquias P, Hass V, Matos TP, Lourenço L, Reis A, et al. The role of copper nanoparticles in an etch-and-rinse adhesive on antimicrobial activity, mechanical properties and the durability of resin-dentine interfaces. *J. Dent.*, 2017;61:12-20.
26. Sousa BC, Massar CJ, Gleason MA, Cote DL. On the emergence of antibacterial and antiviral copper cold spray coatings. *J. Biol. Eng.* 2021;15(1):8.
27. Sterzenbach T, Helbig R, Hannig C, Hannig M. Bioadhesion in the oral cavity and approaches for biofilm management by surface modifications. *Clin. Oral Investig.* 2020;24(12):4237-60.
28. Rudnik LAC, Farago PV, Budel JM, Lyra A, Barboza FM, Klein T, Kanunfre CC, et al. Co-Loaded Curcumin and Methotrexate Nanocapsules Enhance Cytotoxicity against Non-Small-Cell Lung Cancer Cells. *Molecules.* 2020;25:2-19.
29. Lanza CR, De Souza Costa CA, Furlan M, Alecio A, Hebling J. Transdental diffusion and cytotoxicity of self-etching adhesive systems. *Cell Biol. Toxicol.* 2009;25(6):533-43.
30. Sengün A, Yalçın M, Ülker HE, Öztürk B, Hakkı SS. Cytotoxicity evaluation of dentin bonding agents by dentin barrier test on 3-dimensional pulp cells. *Oral Surg Oral Med Oral Pathol Oral Radiol Endod.* 2011;112(3):e83–e88.
31. Cavalcanti BN, Bärschneider LR, Marques MM. Cytotoxicity of substances leached from a conventional and a selfetching adhesive system on human pulp fibroblasts. *Braz Dent Sci.* 2010;13(2):10-4.
32. Elias ST, dos Santos AF, Garcia FCP, Pereira PNR, Hilgert LA, Fonseca-Bazzo YM, et al. Cytotoxicity of Universal, Self-Etching and Etch-and-Rinse Adhesive Systems According to the Polymerization Time. *Braz. Dent. J.* 2015;26(2):160-8.



© 2022 by the authors. Submitted for possible open access publication under the terms and conditions of the Creative Commons Attribution (CC BY NC) license (<https://creativecommons.org/licenses/by-nc/4.0/>).